Supporting Information

Base-Resolution Analysis of 5-Hydroxymethylcytidine by Selective Oxidation and Reverse Transcription Arrest

Kenta Koyama,[a] Gosuke Hayashi,[b] Hiroki Ueda,[c] Satoshi Ota,[c] Genta Nagae,[c] Hiroyuki Aburatani,[c] Akimitsu Okamoto*,[a, c]

[a]Department of Chemistry and Biotechnology, The University of Tokyo, 7-3-1 Hongo, Bunkyo-ku, Tokyo 113-8656, Japan

[b]Department of Biomolecular Engineering, Nagoya University, Furo-cho, Chikusa-ku, Nagoya 464-8603, Japan

[c]The Research Center for Advanced Science and Technology, The University of Tokyo, 4-6-1 Komaba, Meguro-ku, Tokyo 153-8904, Japan

*** Corresponding author:**

E-mail: okamoto@chembio.t.u-tokyo.ac.jp

Tel: +813-5452-5200

Fax: +813-5452-5209

Table S1. DNA/RNA sequences used in this paper.

DNA/RNA	Sequence	Figure
RNA1(X)	5’ -A**X**A-3’ (**X** = ^{hm5}C or C)	Fig. 2, S1-2
RNA2(X)	5’ -CACU**X**GCUUCCUCCAGAUGA-3’ (**X** = ^{hm5}C)	Fig. 3, 4, S1, S3-6
Primer DNA1	5’ -Fluorescein-TCATCTGGAGGA-3’	Fig. 3, S6
Primer DNA2	5’ -Fluorescein-TCATCTGGAGGAAGC-3’	Fig. S3
Primer DNA3	5’ -Fluorescein-TCATCTGGAGGAAG-3’	Fig. S4, S6
Cleaved RNA control	5’ -GCUUCCUCCAGAUGA-3’	Fig. S5
Linker DNA	5’ -rAppCTGTAGGCACCATCAAT/3ddC/-3’	Fig. 4
RT primer	5’ -/Phos/AGATCGGAAGAGCGTCGTGTAGGGAAAGAG TGTAGATCTCGGTGGTCGC/SpC18/CACTCA/SpC18/TT CAGACGTGTGCTCTTCCGATCTATTGATGGTGCCTAC AG-3’	Fig. 4, 5
PCR primers	5’ -AATGATACGGCGACCACCGAGATCTACAC-3’ 5’ -CAAGCAGAAGACGGCATACGAGAT/NNNNNN/GTGA CTGGAGTTCAGACGTGTGCTCTTCCG-3’	Fig. 4, 5
RNA3(X)	5’ -GGGAGGUGAGAGUGAGAGUAUGUAUAGAAUUGA UAU**X**GAAAUGAGUAGGUGAUGGAAGUGGUAGGUAA GGGAA-3’ (**X** = ^{hm5}C, ^{m5}C, or C)	Fig. S7
RNA4	5’ -GGGGUAGGAUGUGUGAUGAGAAA**^{hm5}C**UUAUAAG GAGUAAUGUGGGAUGUGUAGAGGAUUAGAUUAUGA GGUAGAUUGUGAUAUGAAGUGGAGAGUGAUGAGUG GUAAGGGAAUGAGUGGAAAUGA-3’	Fig. 5
RNA5	5’ -GGGGUAUGAUGUAUGAGGAGAAA**C**UUAUGAGGA GUGAUGUGGGAUGUUGAGAAGAUUGAUUAAUGAGG AGUAUUGUGAUAGUAAGGUAGAGGUGGUAGUAGGU AAGGAGUAGAUGGGAAUGAA-3’	Fig. 5

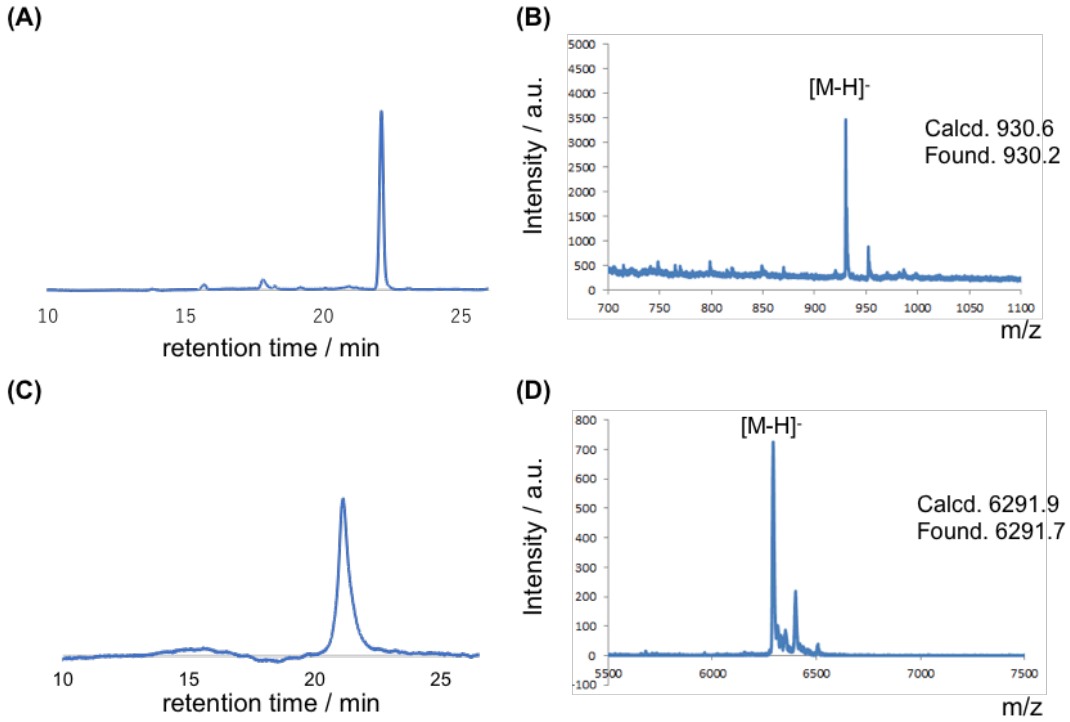

Fig. S1 HPLC traces and MALDI-TOF MS data of synthesized ^{hm5}C-containing oligonucleotides. Purified RNA1(^{hm5}C) and RNA2(^{hm5}C) was analyzed by HPLC (A and C) and MALDI-TOF-MS (B and D), respectively.

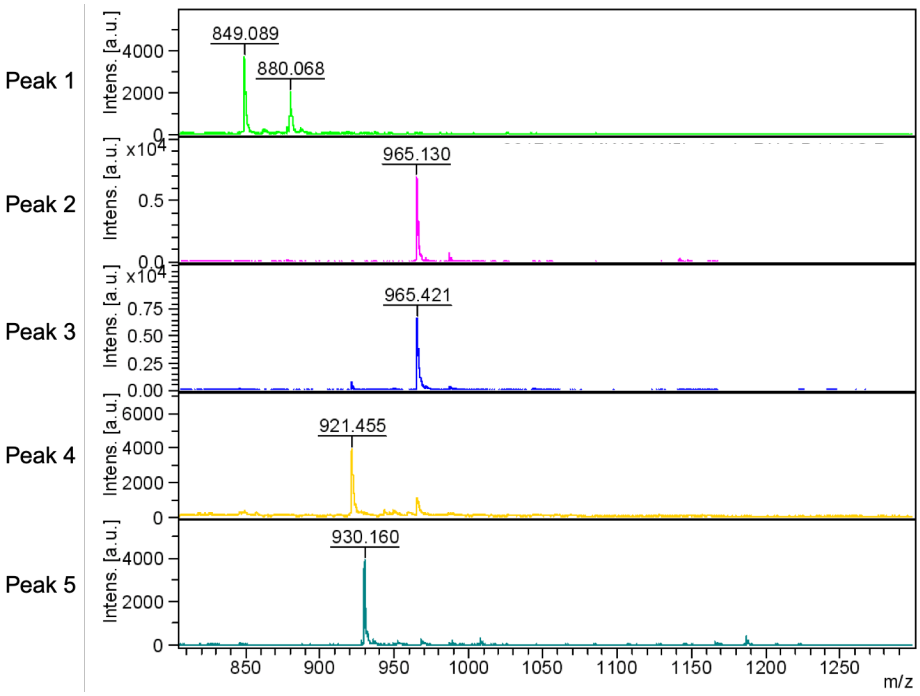

Fig. S2 MALDI-TOF MS charts of HPLC-purified products derived from RNA1(^{hm5}C) after 1-h incubation with peroxotungstate. The chromatogram of each peak was shown in Fig. 1(A).

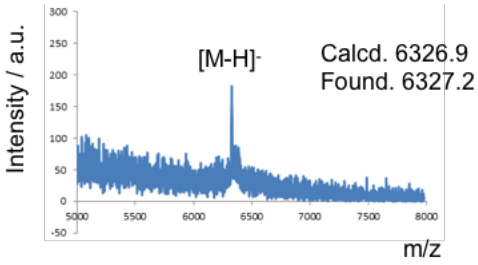

Fig. S3 RNA2(^{hm5}C) was monitored by MALDI-TOF-MS after the incubation at 50 °C with peroxotungstate. Oxidized RNA2(^{hm5}C) showed mass of thT-containing RNA2 (thT).

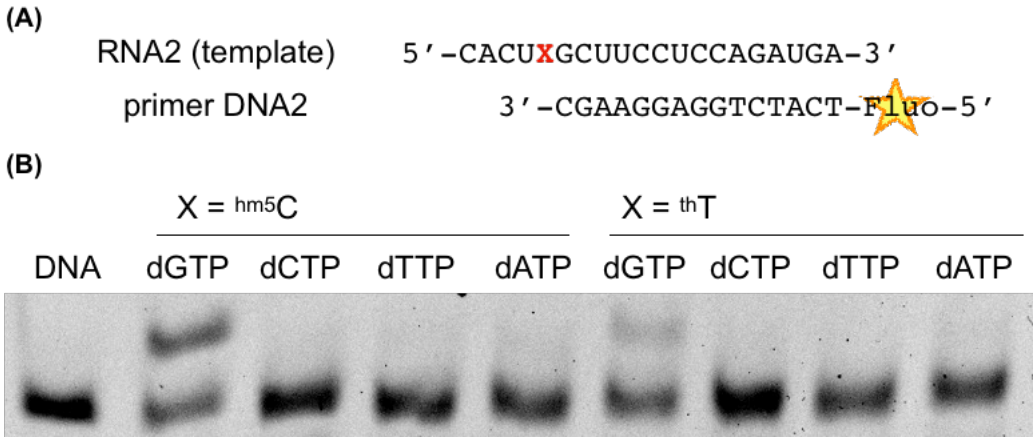

Fig. S4 (A) RNA2 (X = ^{hm5}C or thT) before or after peroxotungstate-oxidation was hybridized with primer DNA2 and reverse-transcribed in the presence of dATP, dGTP, dCTP, or dTTP. (B) Denaturing PAGE analysis of reverse-transcribed products. Incorporation of dNTPs into fluorescein-labeled primer DNA2 hybridized with template RNA2(^{hm5}C) or RNA2(thT) was analyzed.

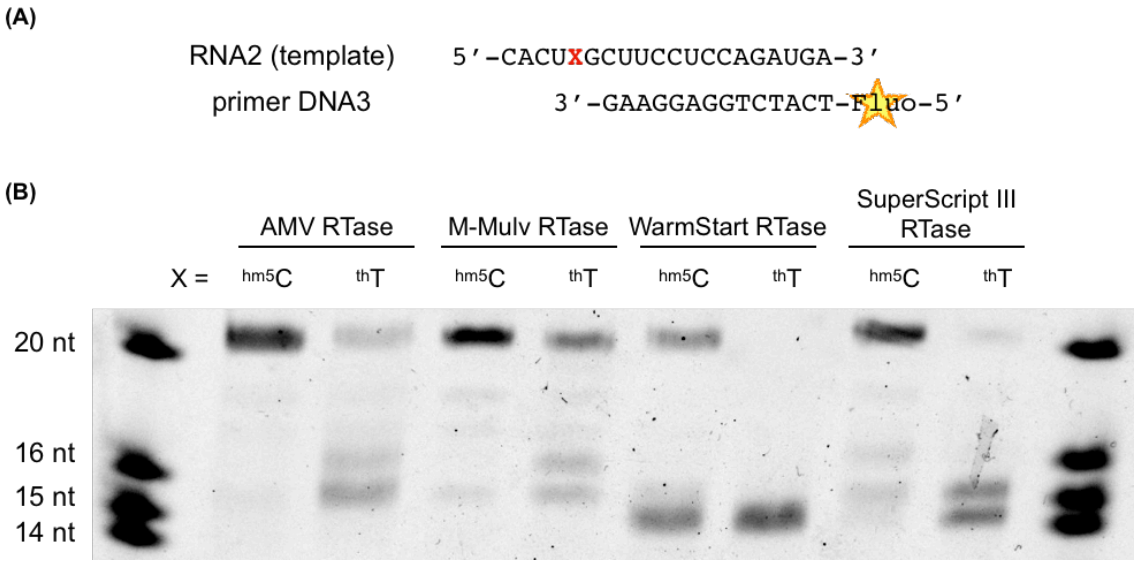

Fig. S5 (A) The 14-nt fluorescein-labeled primer DNA3 was hybridized to 20-nt template RNA2(X = ^{hm5}C or thT) and elongated using several reverse transcriptases. (B) Denaturing PAGE analysis of the reverse-transcribed product using several reverse transcriptases: AMV reverse transcriptase, M-MuLV transcriptase, WarmStart reverse-transcriptase, and SuperScript III transcriptase. 14, 15, 16, 20-nt oligonucleotides were used as a marker for truncated product.

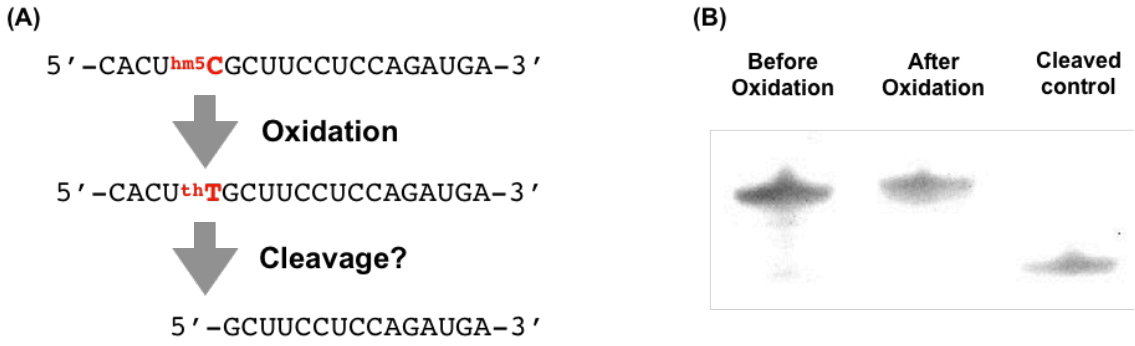

Fig. S6 (A) After the oxidation, 15-nt RNA product may exist if oxidized RNA2 is cleaved at thT site. (B) Denaturing PAGE analysis showed no cleavage in RNA2 after the oxidation with peroxotungstate in 5 hours. 15-nt RNA was used as a marker for cleavage product at the thT site.

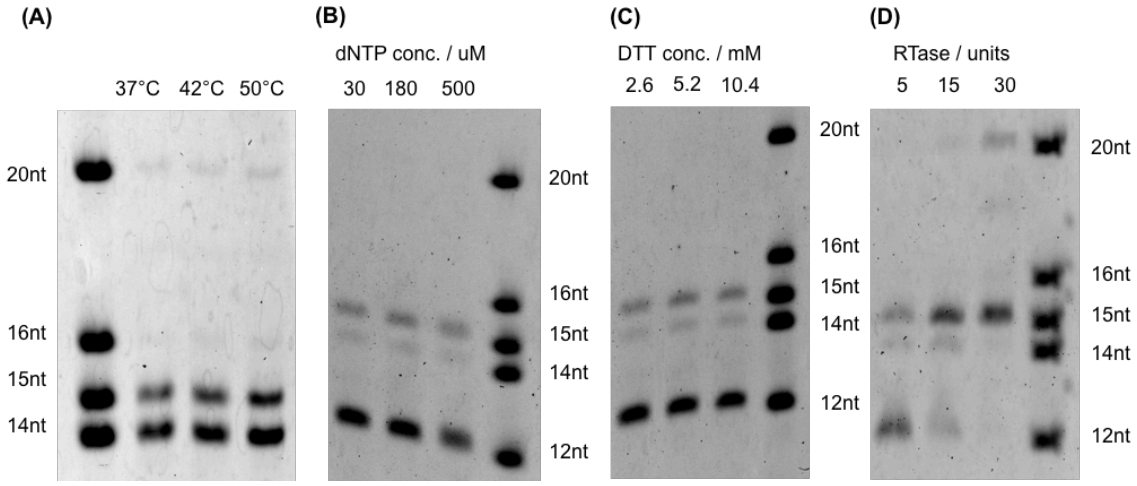

Fig. S7 Optimization of reverse-transcription condition to maximize truncation efficiency. 20-nt RNA2(thT) was hybridized with 12-nt primer DNA1 or 14-nt primer DNA3 and reverse-transcribed using SuperScript III RTase under several conditions. (A) Incubation temperature, (B) dNTP concentration, (C) DTT concentration, and (D) RTase amount were optimized.

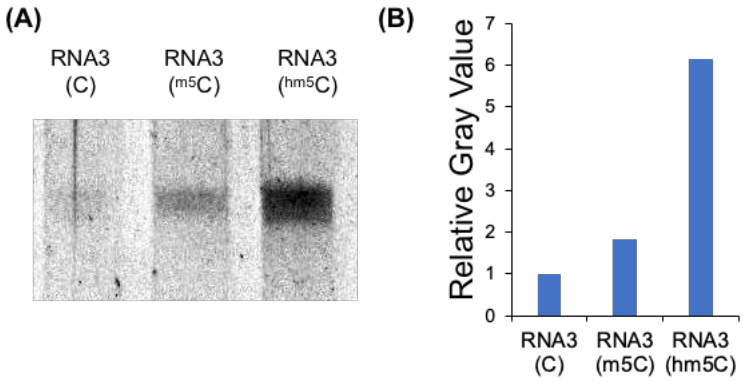

Fig. S8 (A) Denaturing PAGE analysis of immunoprecipitated C, ^{m5}C, or ^{hm5}C-containing RNA3 using polyclonal anti-^{5hm}C antibody (rabbit) with 150 mM sodium chloride in the buffer. (B) The gray value of the gel bands of precipitated RNA3 was analyzed.

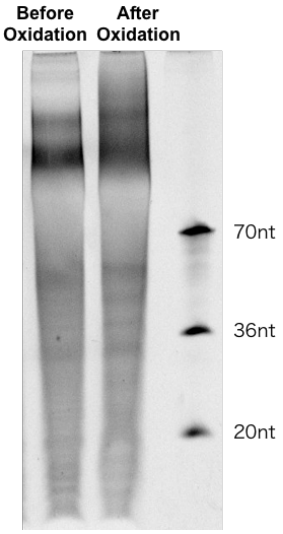

Fig. S9 Denaturing PAGE analysis of ^{hm5}C-containing RNA3 before and after the oxidation with peroxotungstate in 5 hours.

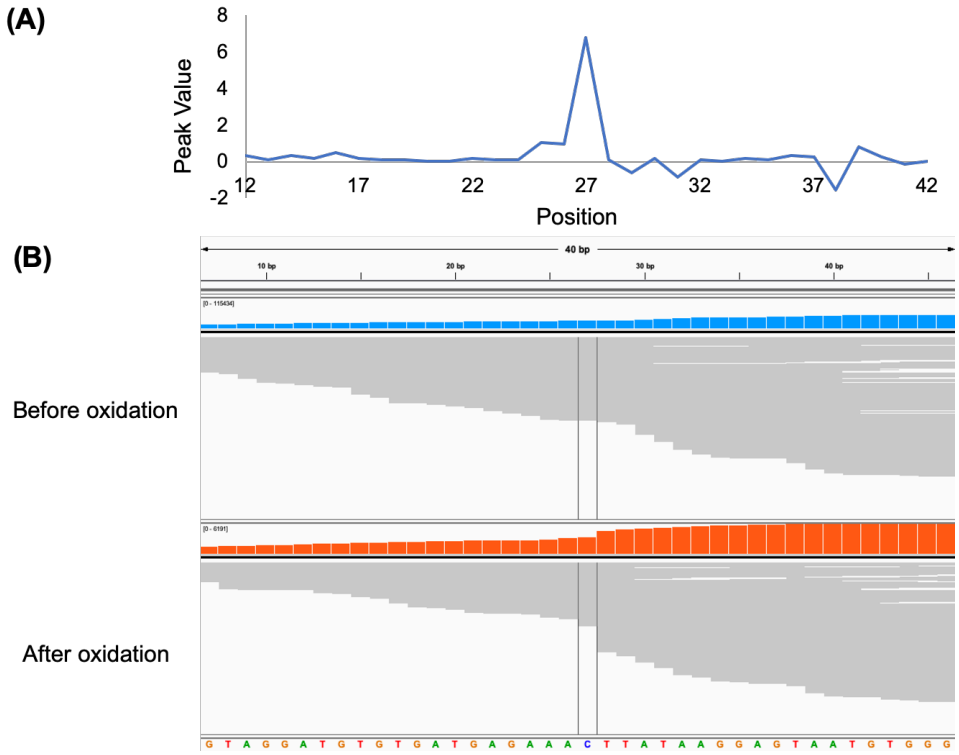

Fig. S10 Peak value and read coverage tracks of RNA4. (A) Peak values around ^{hm5}C position (27th position) in RNA4 showing the highest peak value at the ^{hm5}C position. (B) Read coverage tracks and alignment tracks of RNA4 (top) before and (bottom) after the peroxotungstate-mediated oxidation visualized using Integrative Genomics Viewer (IGV). After the oxidation, the coverage was decreased at the ^{hm5}C position (the center C position), suggesting truncation occurred at the site.

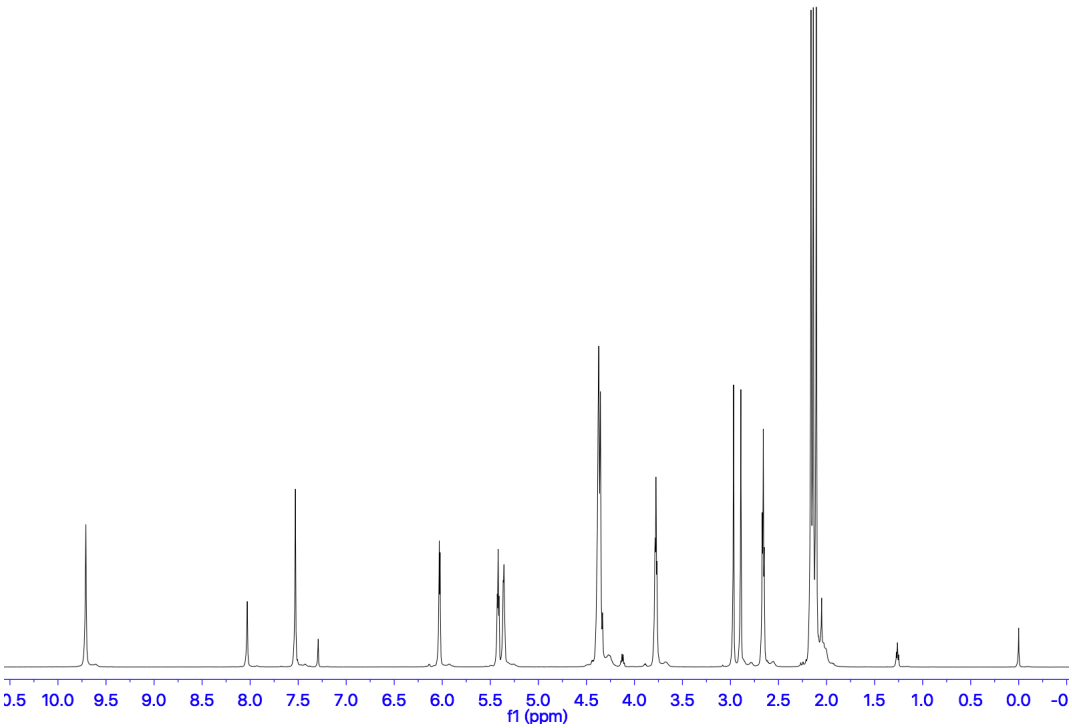

Fig. S11 ^{1}H NMR spectrum of nucleoside **2** in $CDCl_3$.

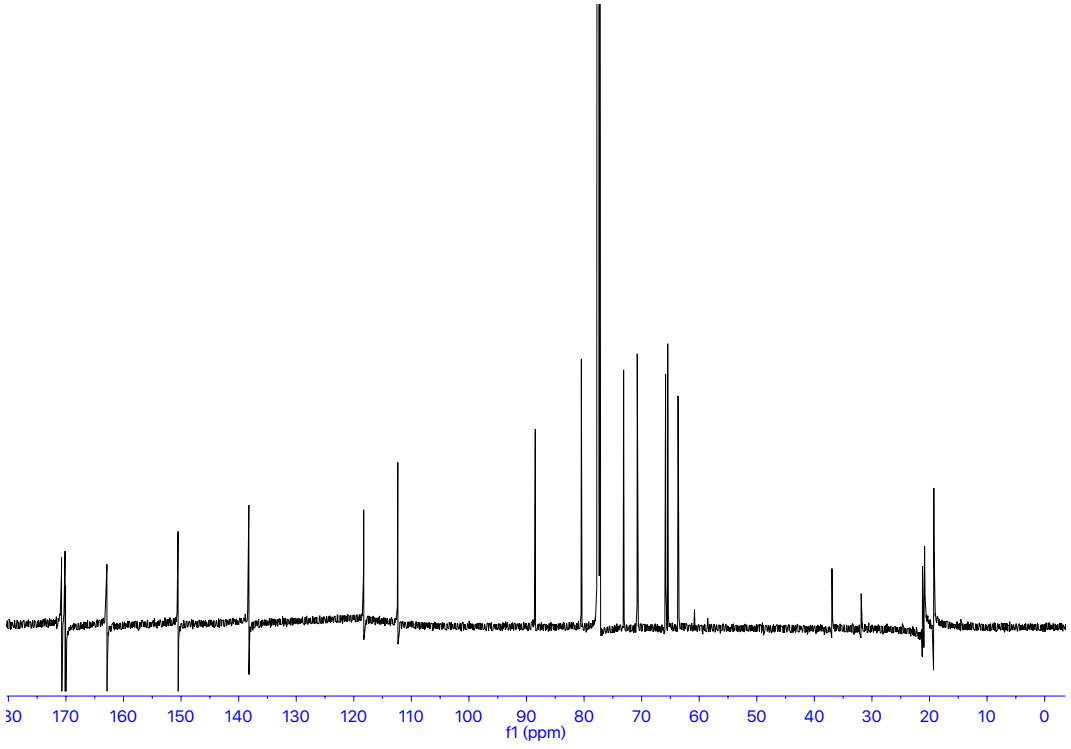

Fig. S12 ^{13}C NMR spectrum of nucleoside **2** in $CDCl_3$.

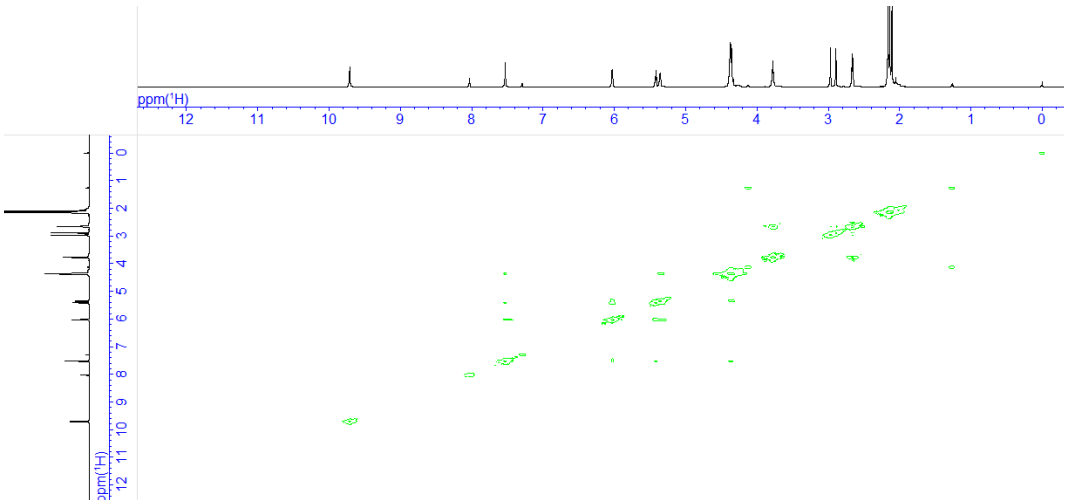

Fig. S13 COSY NMR spectrum of nucleoside **2** in $CDCl_3$.

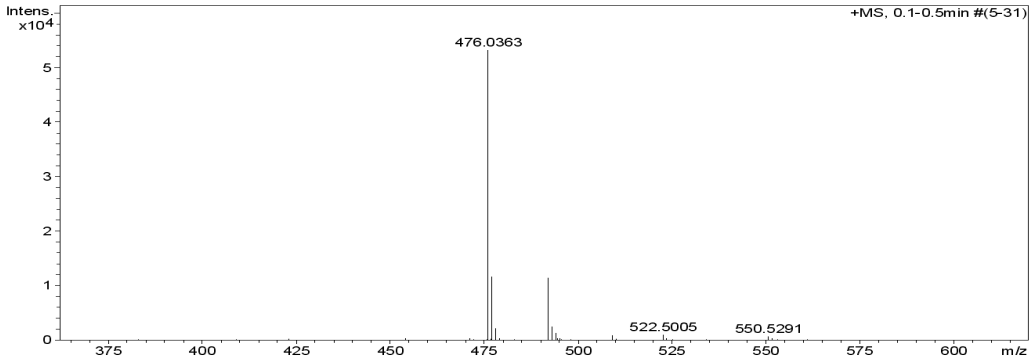

Fig. S14 ESI-MS spectrum of nucleoside **2**.

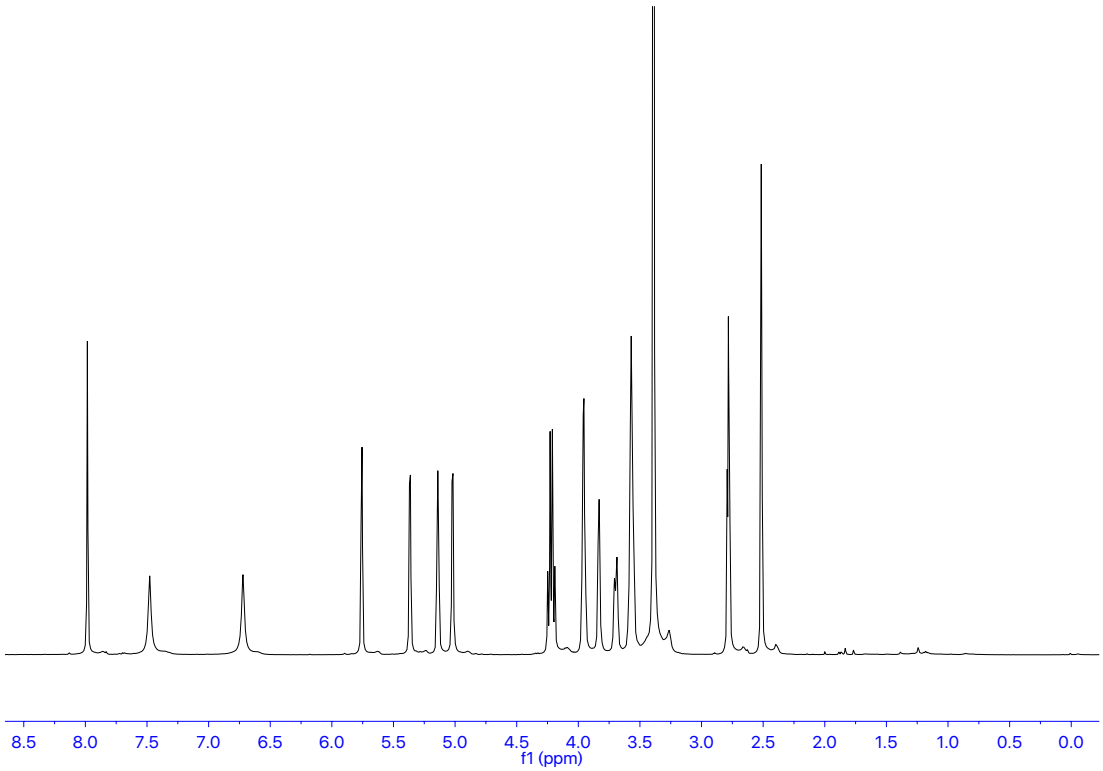

Fig. S15 ^{1}H NMR spectrum of nucleoside **3** in DMSO-d_6.

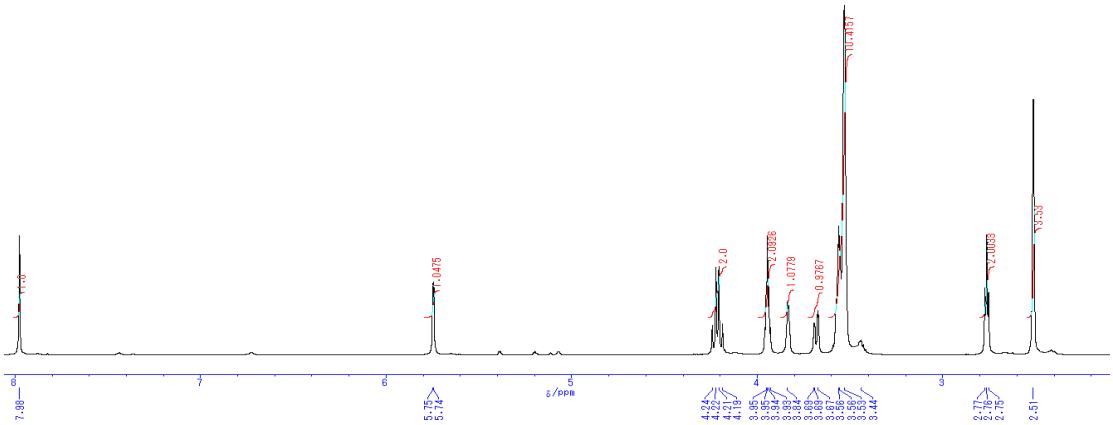

Fig. S16 ^{1}H NMR spectrum of nucleoside **3** in DMSO-d6 with a drop of D_2O.

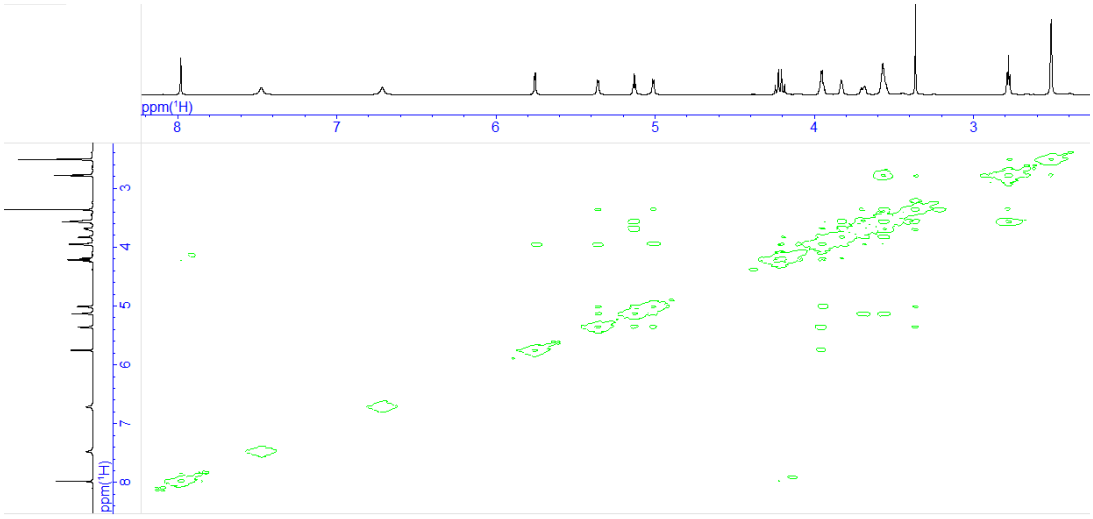

Fig. S17 COSY NMR spectrum of nucleoside **3** in DMSO-d_6.

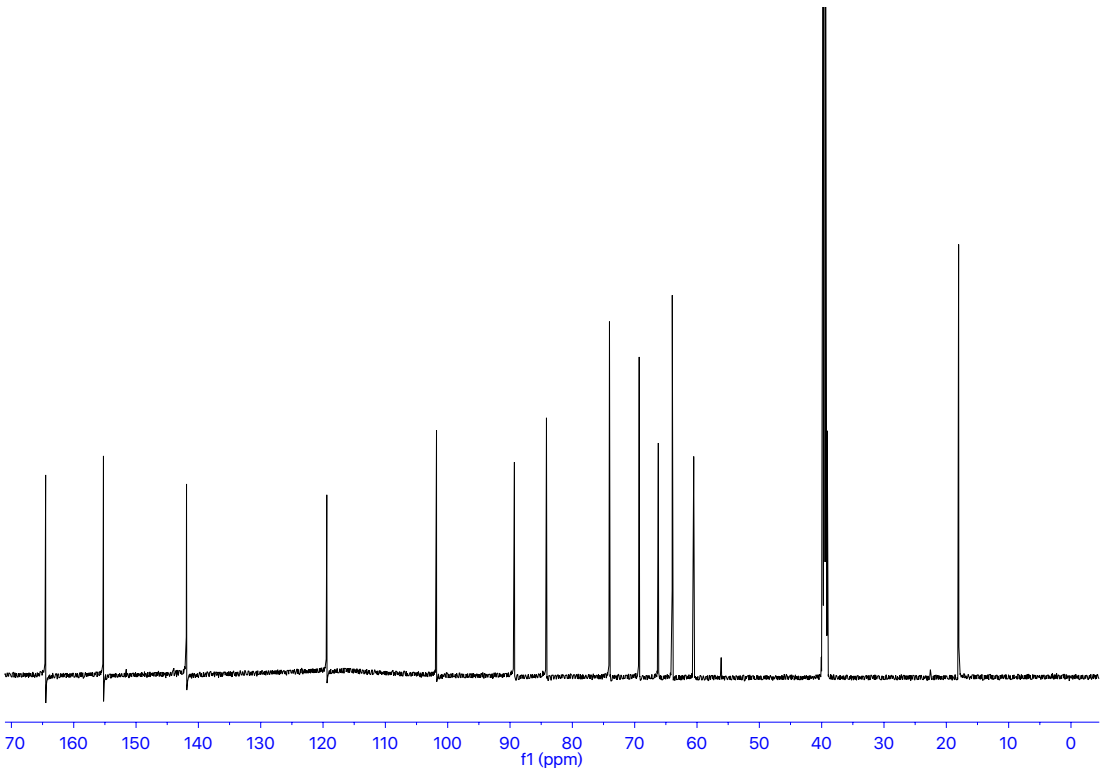

Fig. S18 ^{13}C NMR spectrum of nucleoside **3** in DMSO-d_6.

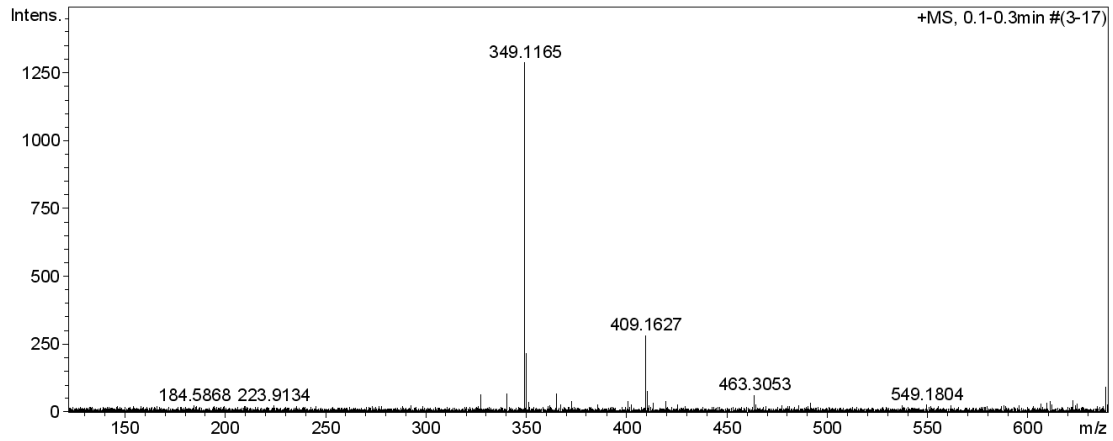

Fig. S19 ESI-MS spectrum of nucleoside **3**.

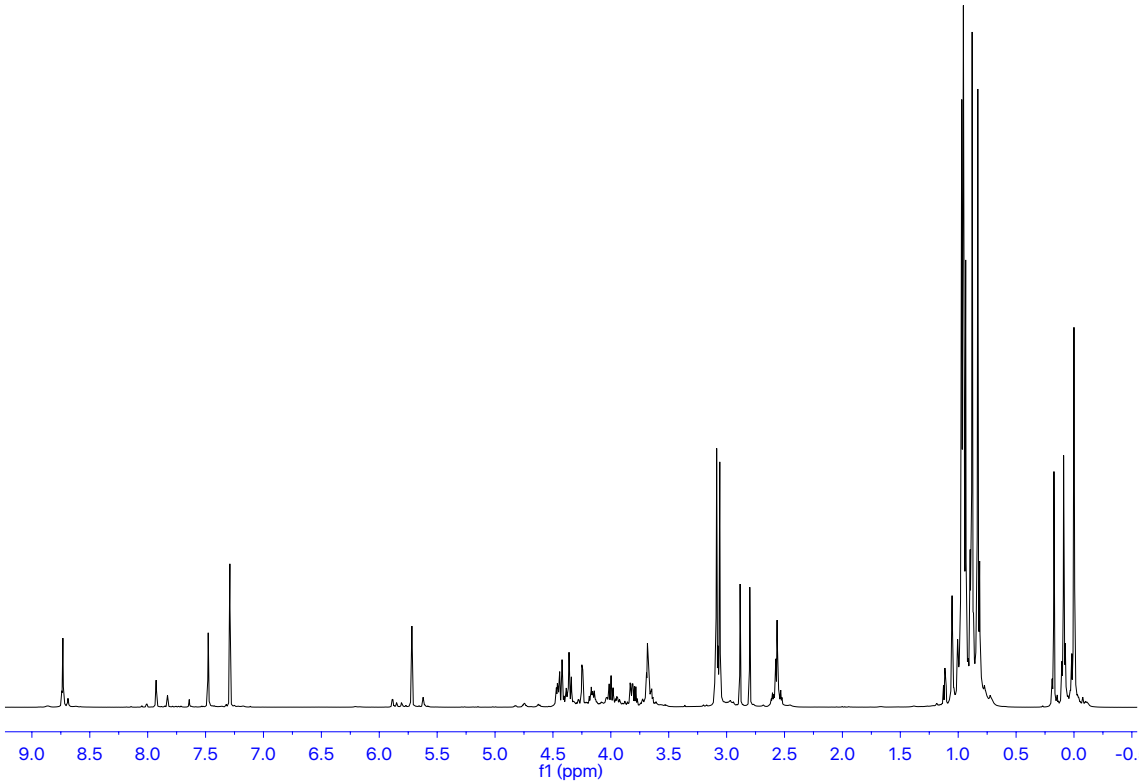

Fig. S20 ^{1}H NMR spectrum of nucleoside **4** in $CDCl_3$.

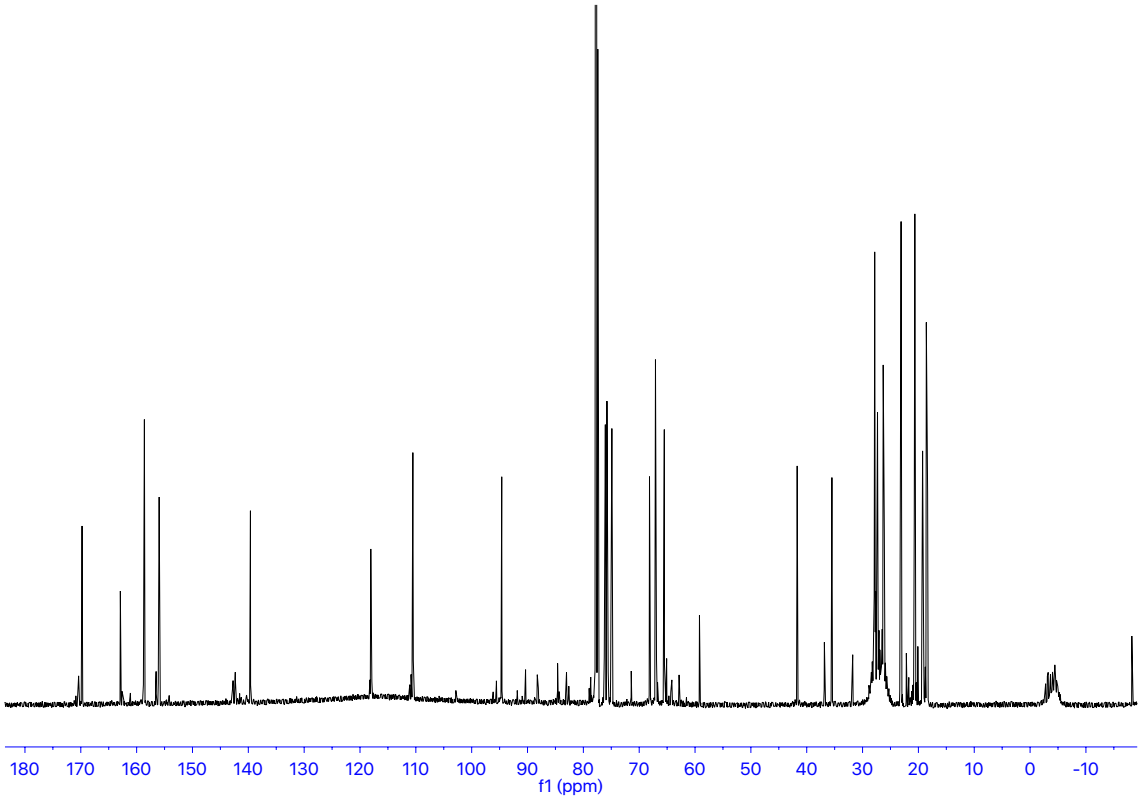

Fig. S21 ^{13}C NMR spectrum of nucleoside **4** in $CDCl_3$.

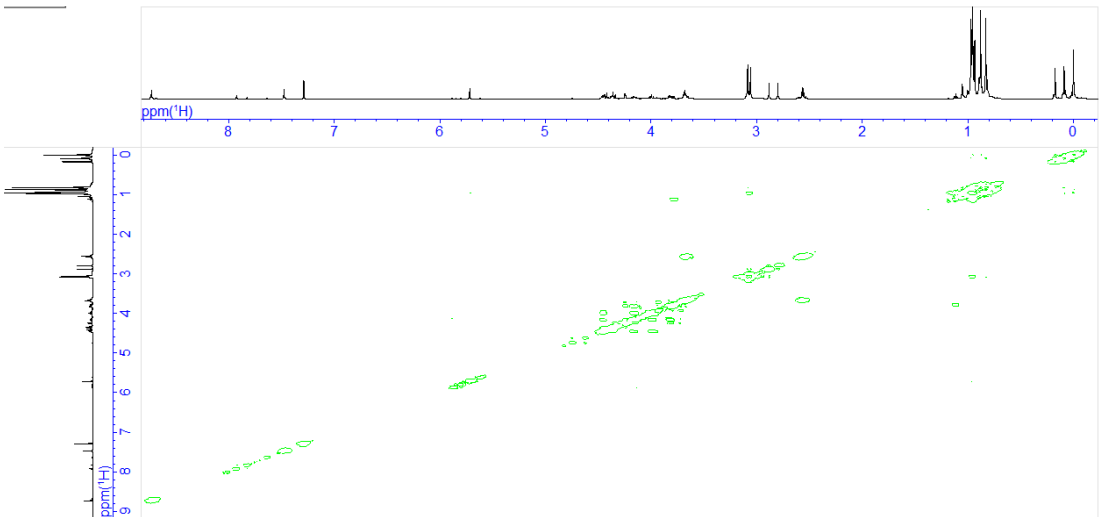

Fig. S22 COSY NMR of nucleoside **4** in $CDCl_3$.

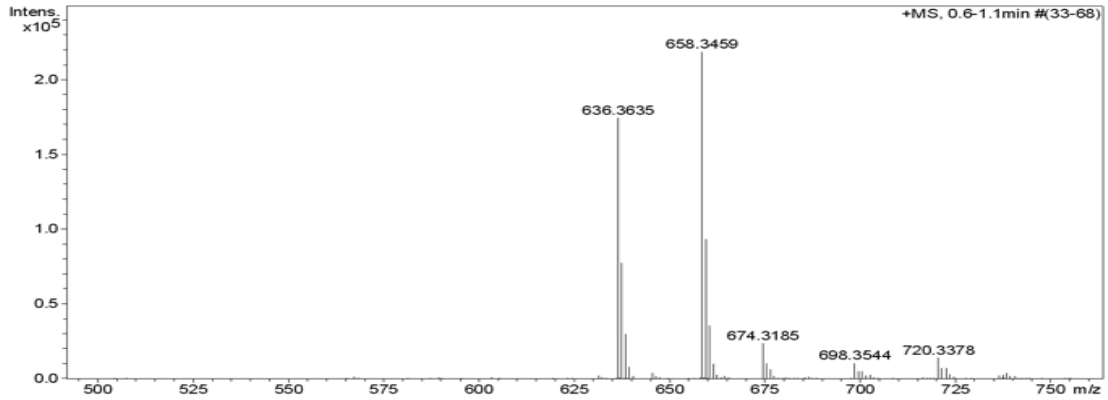

Fig. S23 ESI-MS spectrum of nucleoside **4**.

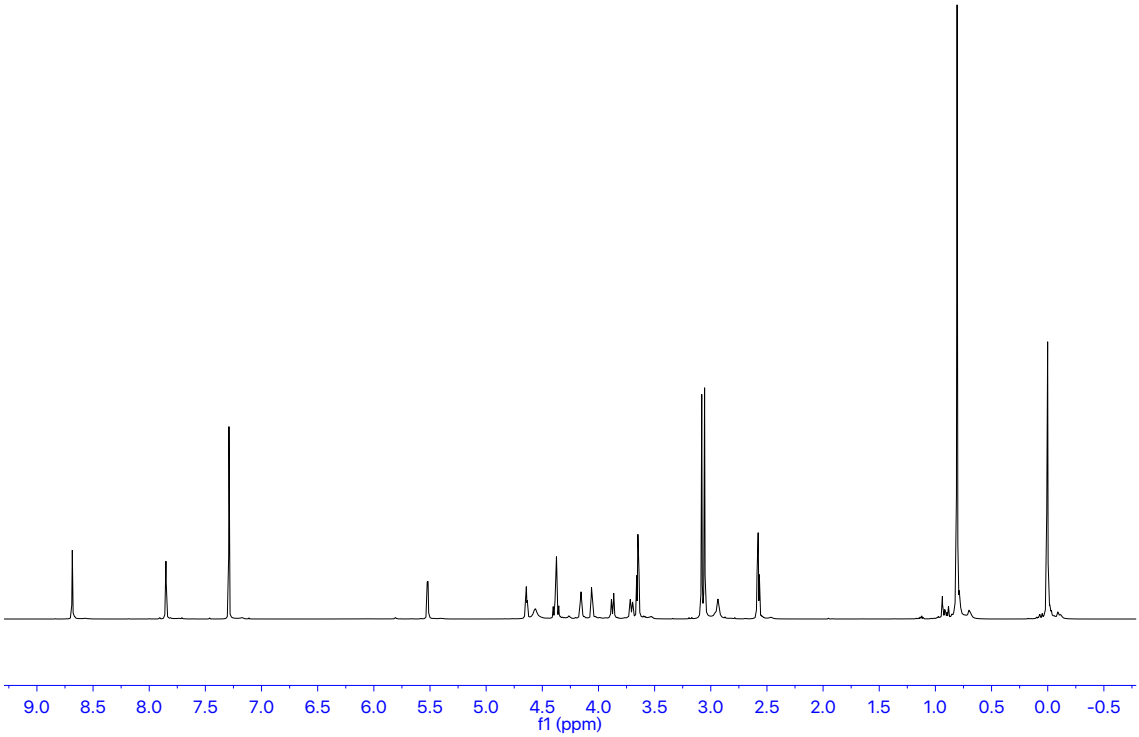

Fig. S24 ^{1}H NMR spectrum of nucleoside **5** in $CDCl_3$.

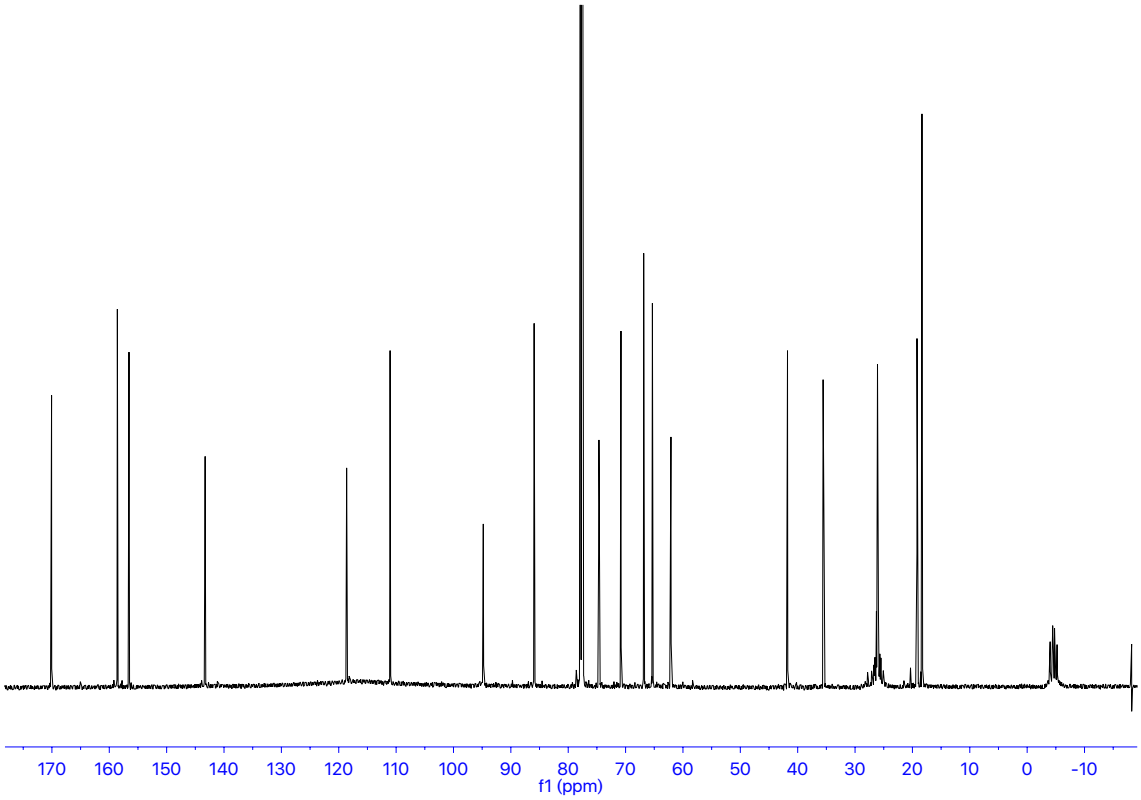

Fig. S25 ^{13}C NMR spectrum of nucleoside **5** in $CDCl_3$.

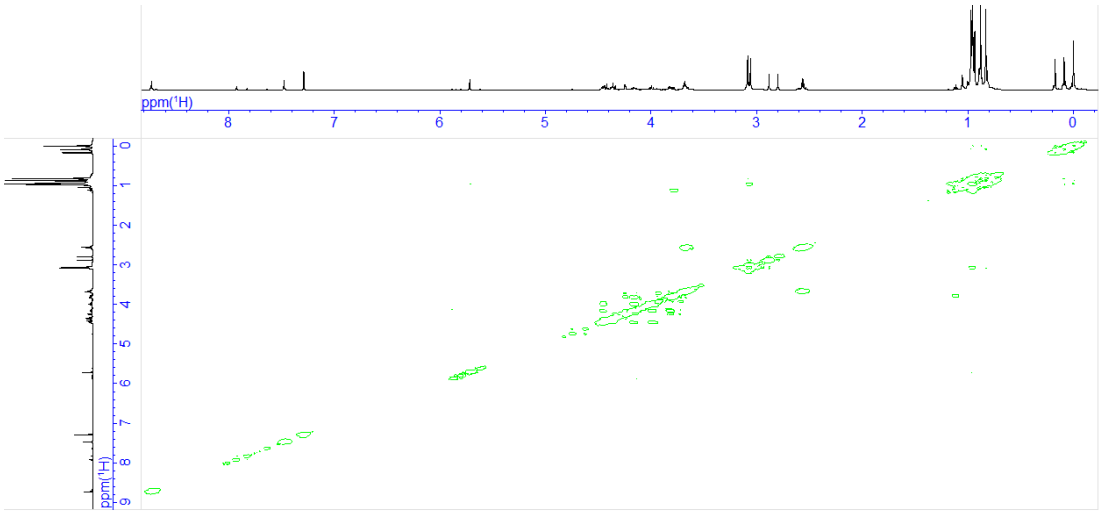

Fig. S26 COSY NMR of nucleoside **5** in DMSO-d_6.

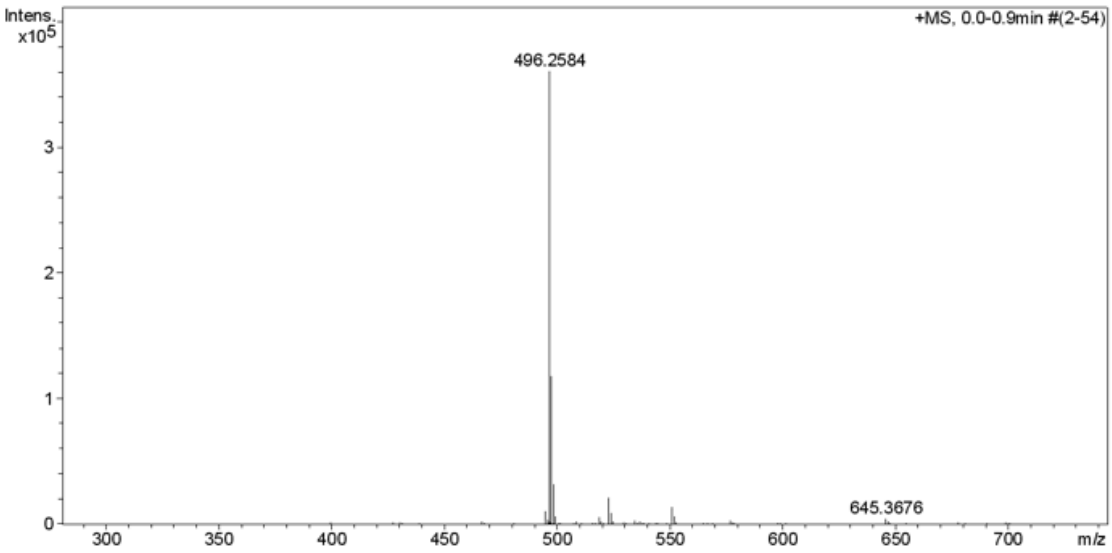

Fig. S27 ESI-MS spectrum of nucleoside **5**.

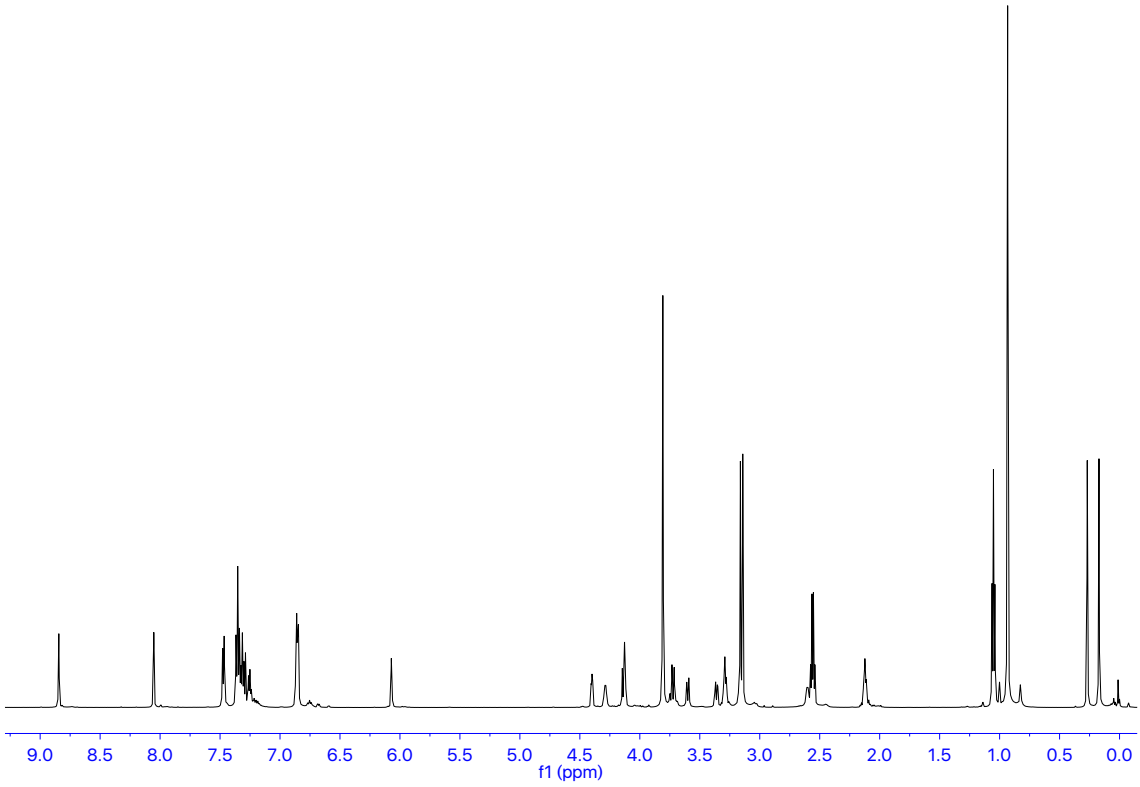

Fig. S28 ^{1}H NMR spectrum of nucleoside **6** in $CDCl_3$.

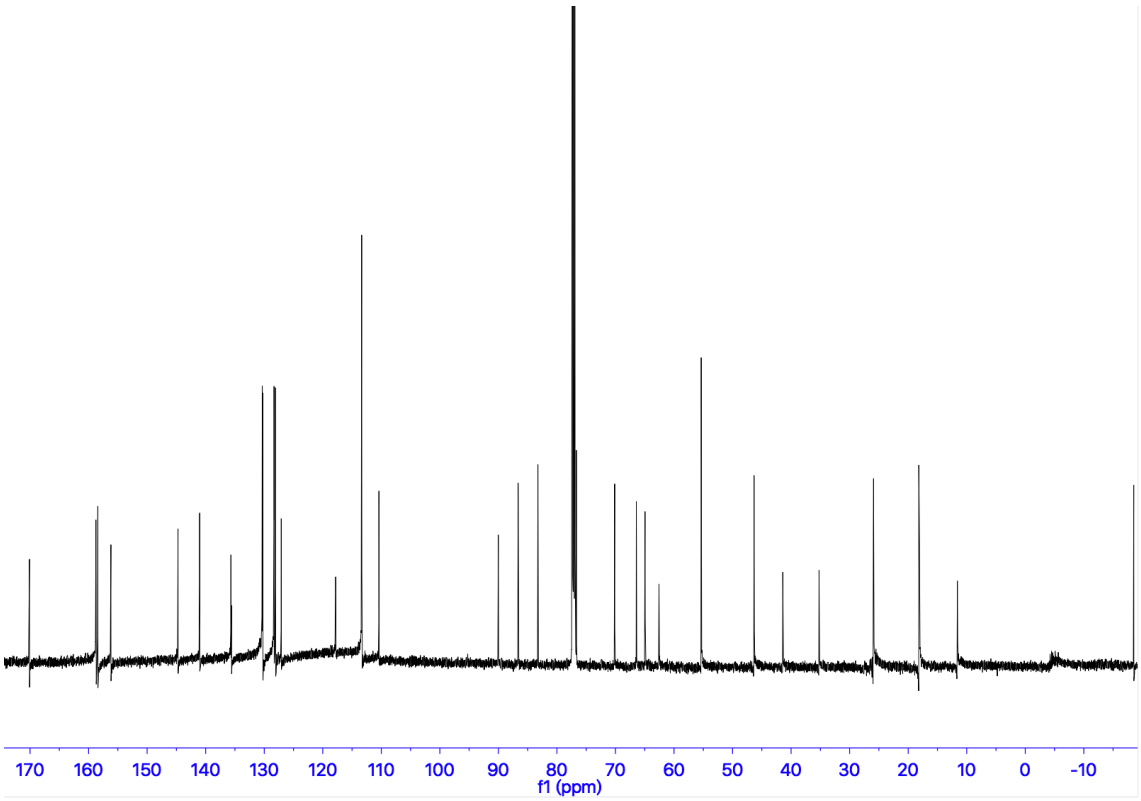

Fig. S29 ^{13}C NMR spectrum of nucleoside **6** in $CDCl_3$.

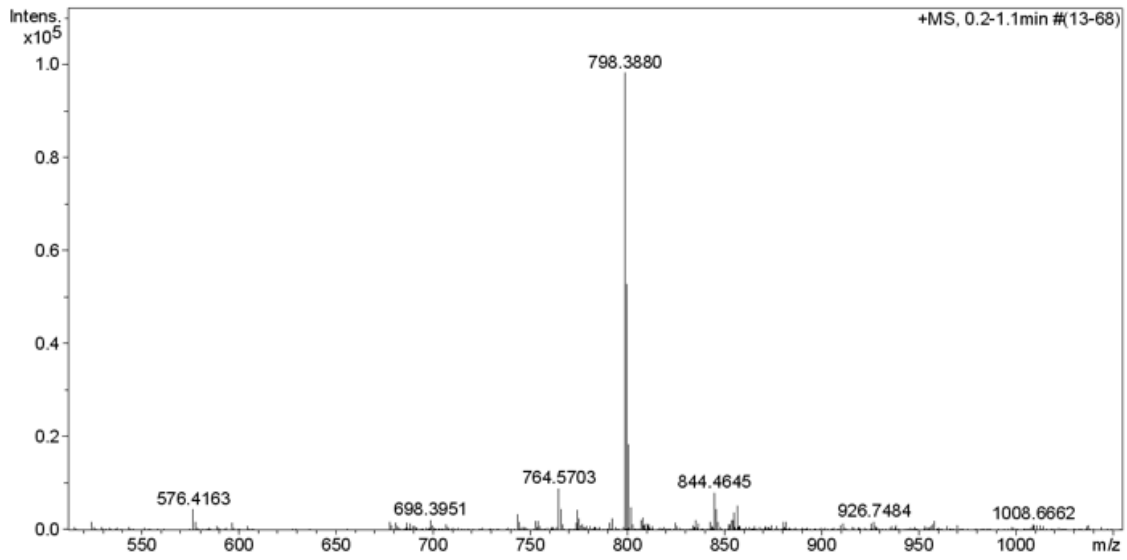

Fig. S30 ESI-MS spectrum of nucleoside **6**.

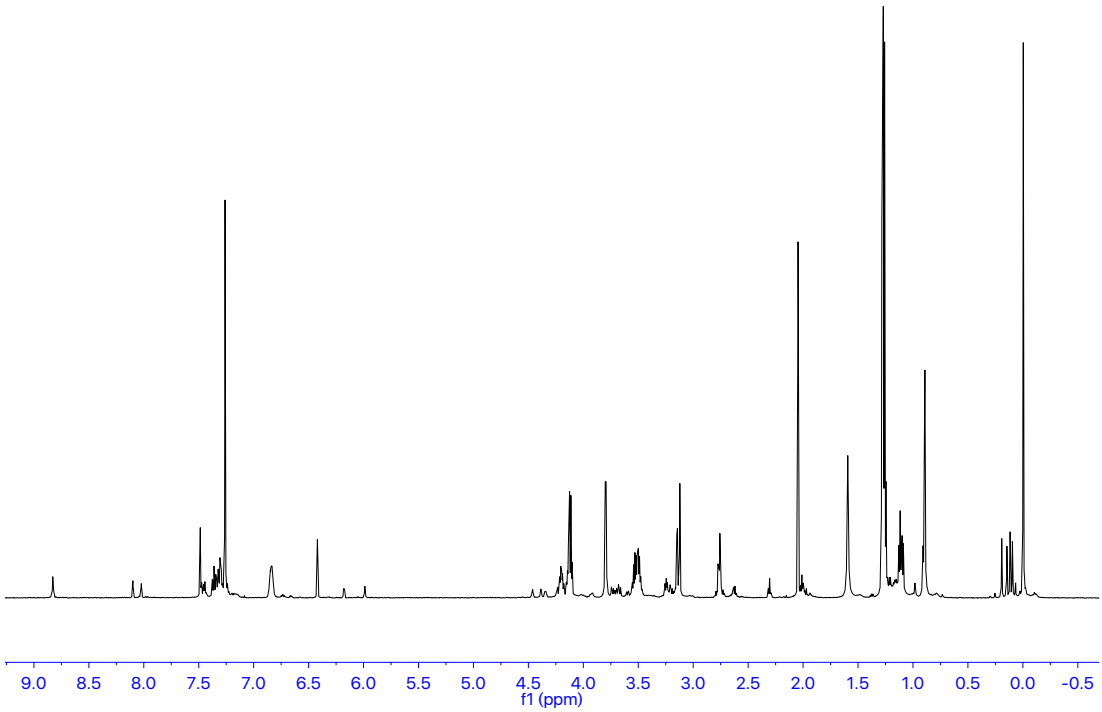

Fig. S31 ^{1}H NMR spectrum of phosphoramidite **7** in $CDCl_3$.

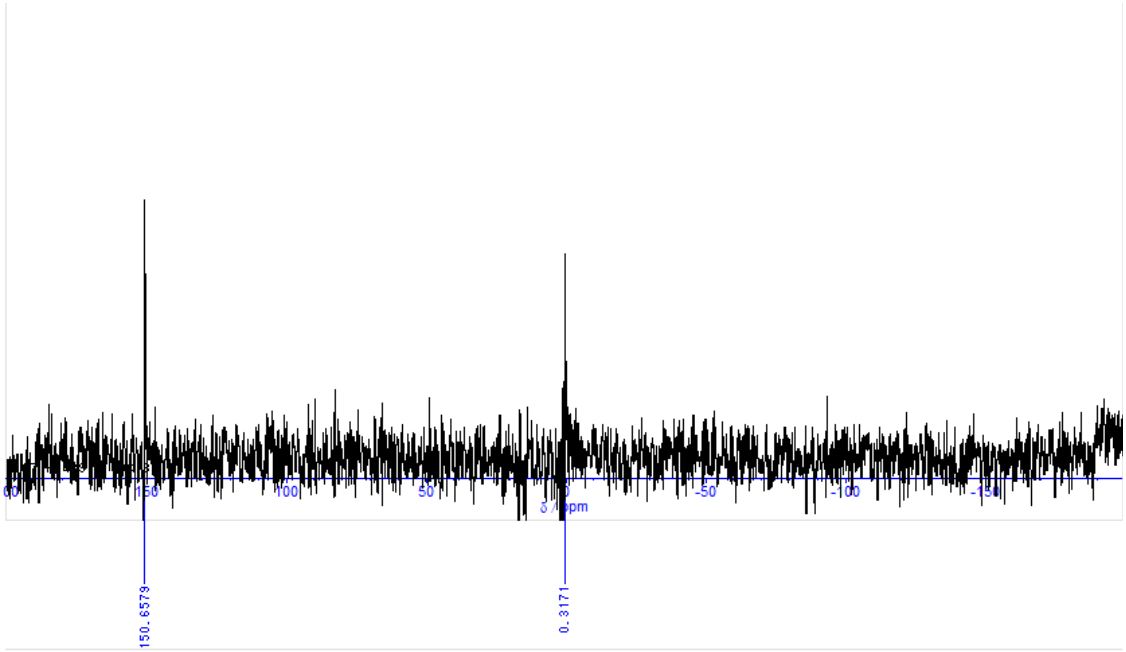

Fig. S32 ^{31}P NMR spectrum of nucleoside **7** in $CDCl_3$.

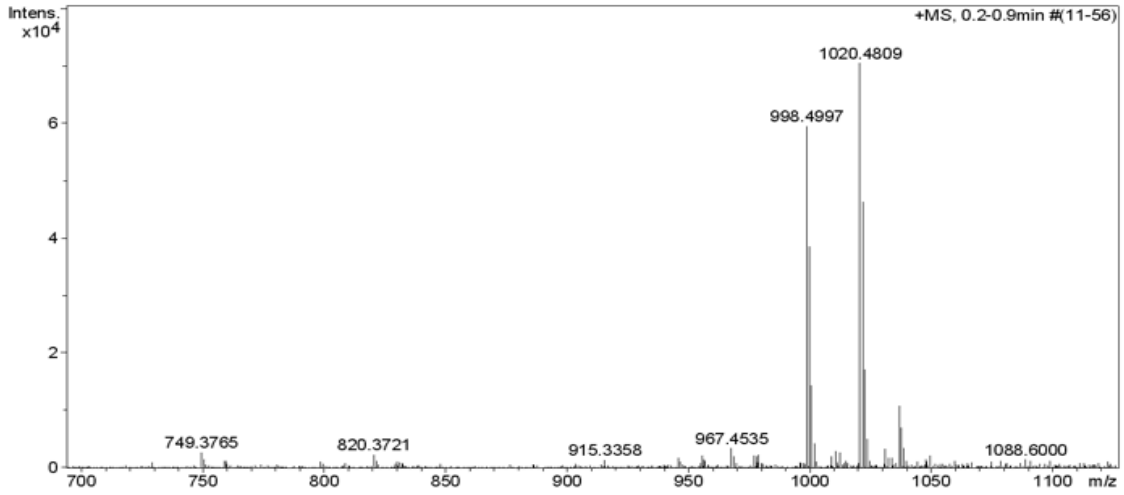

Fig. S33 ESI-MS spectrum of nucleoside **7**.